

# ADVANCED MATERIALS

## Supporting Information

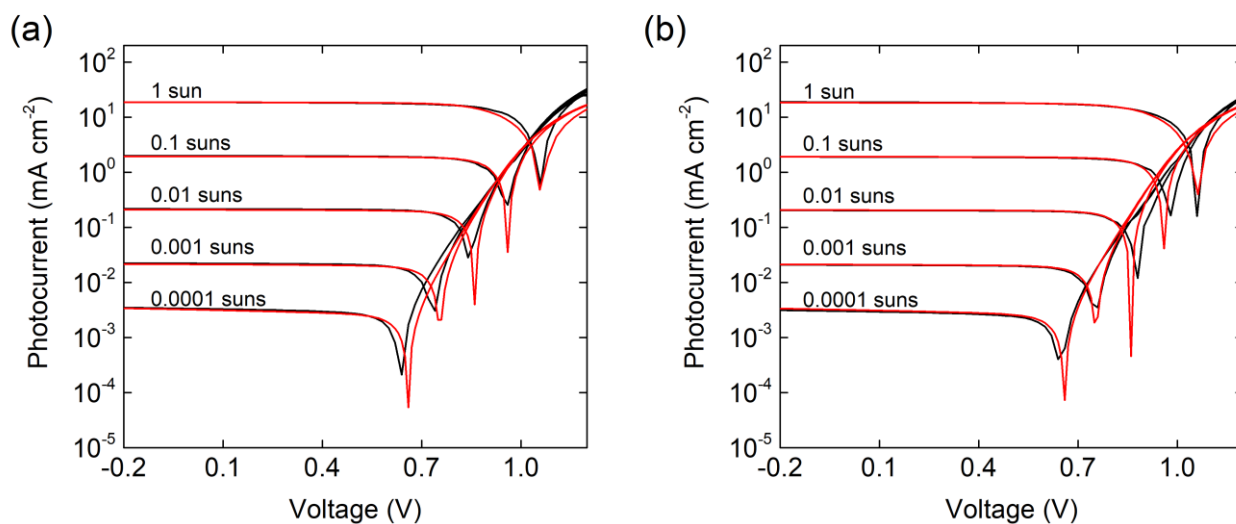
for *Adv. Mater.*, DOI: 10.1002/adma.202105920

Light Intensity Analysis of Photovoltaic Parameters for  
Perovskite Solar Cells

*Damian Glowienka and Yulia Galagan\**

## Supporting Information

## Light intensity analysis of photovoltaic parameters for perovskite solar cells

*Damian Glowienka, Yulia Galagan\**

**Figure S1.** The experimental (black line) and simulation (red line) results for PSC measured under different light intensities for the devices with (a) front and (b) rear illumination.

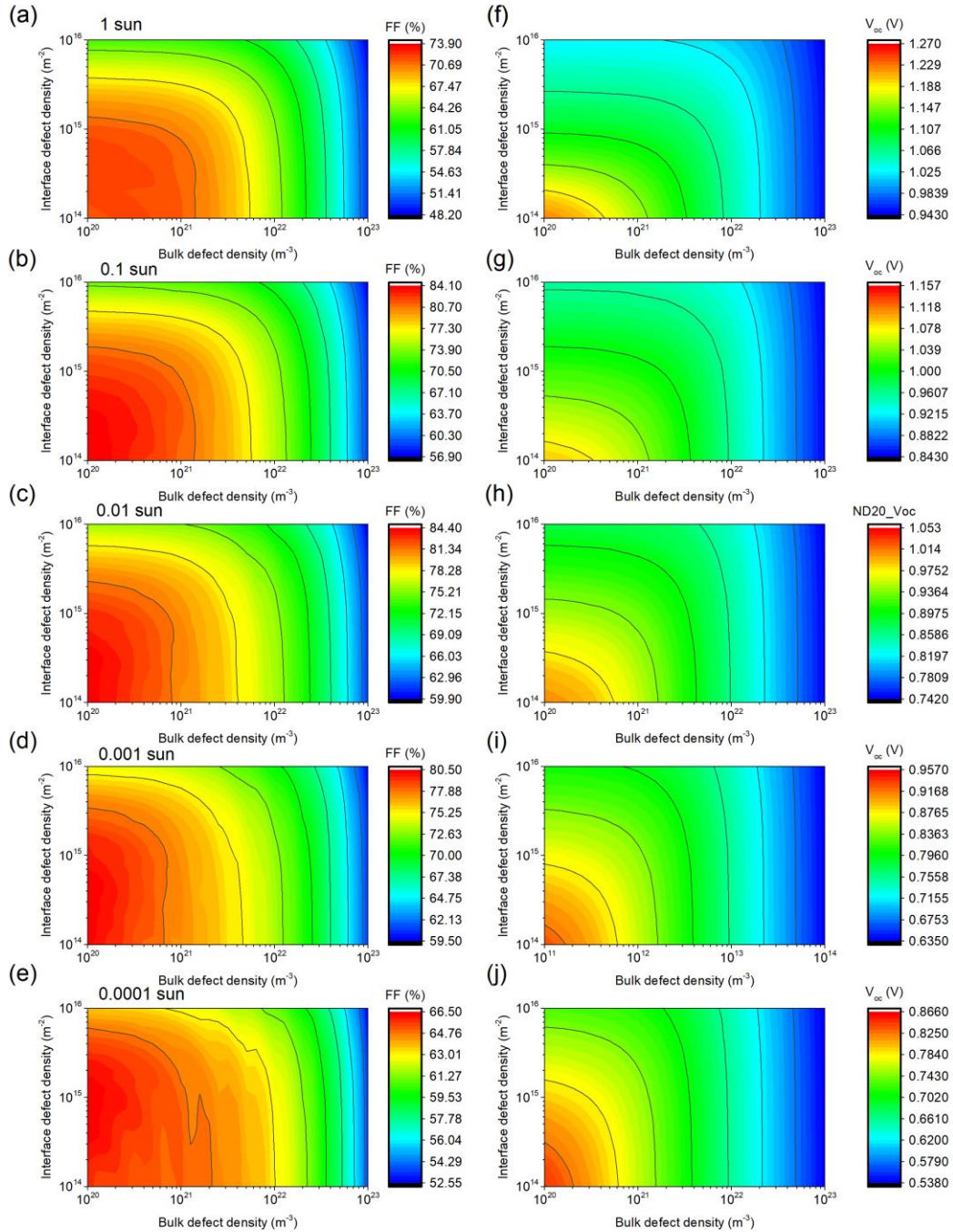


**Figure S2.** 3-D graphs of light intensity-dependent FF and  $V_{oc}$  in the semitransparent PSC with rear illumination considering different levels of bulk and interface defect densities, responsible for bulk and interface recombination. Here the bulk defect densities are in the range of  $10^{20} \text{ m}^{-3}$  to  $10^{23} \text{ m}^{-3}$ . The interface defect densities are symmetric for both interfaces and in the range of  $10^{14} \text{ m}^{-2}$  to  $10^{16} \text{ m}^{-2}$ .

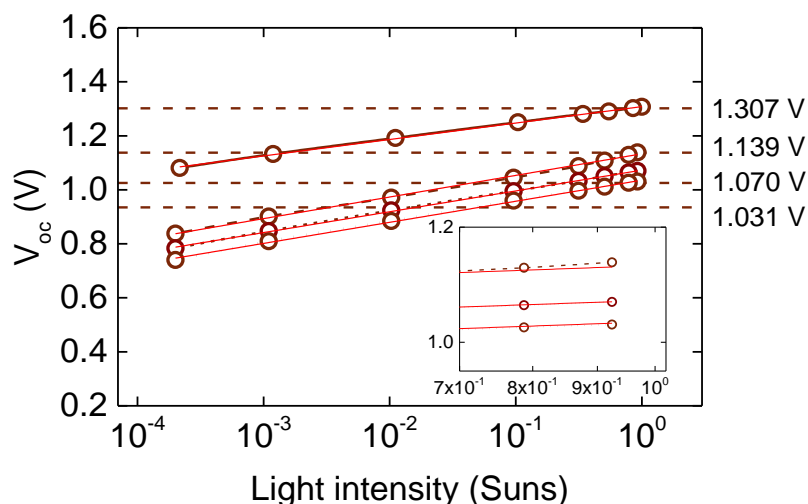


**Figure S3.** Simulated results for  $V_{oc}$  of PSCs with front side illumination under different light intensities. The simulated devices having only interface recombination as a performance-limiting factor in the devices.

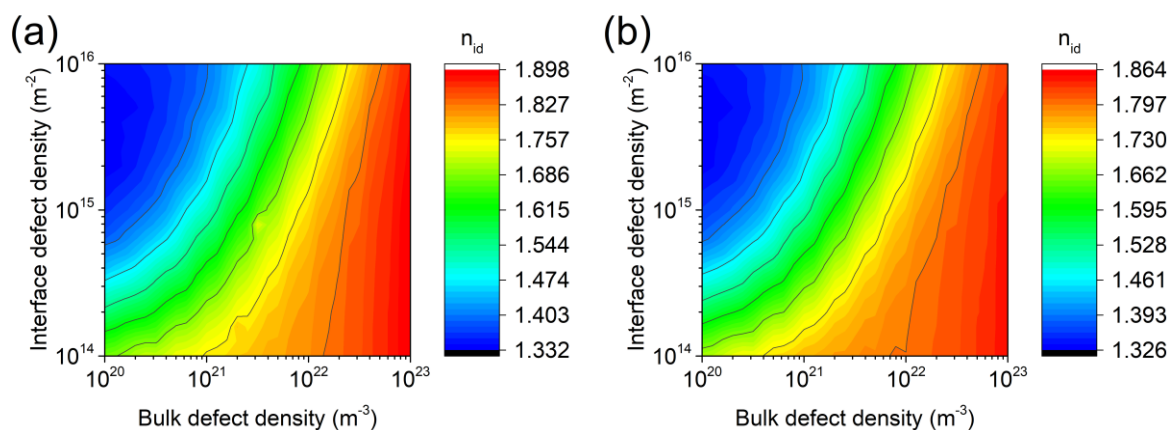


**Figure S4.** 3-D graphs of ideality factors from the front (a) and rear (b) sides of the semitransparent PSC considering different levels of bulk and interface defect densities, responsible for bulk and interface recombination. Here the bulk defect densities are in the range of  $10^{20} \text{ m}^{-3}$  to  $10^{23} \text{ m}^{-3}$ . The interface defect densities are symmetric for both interfaces and in the range of  $10^{14} \text{ m}^{-2}$  to  $10^{16} \text{ m}^{-2}$ .

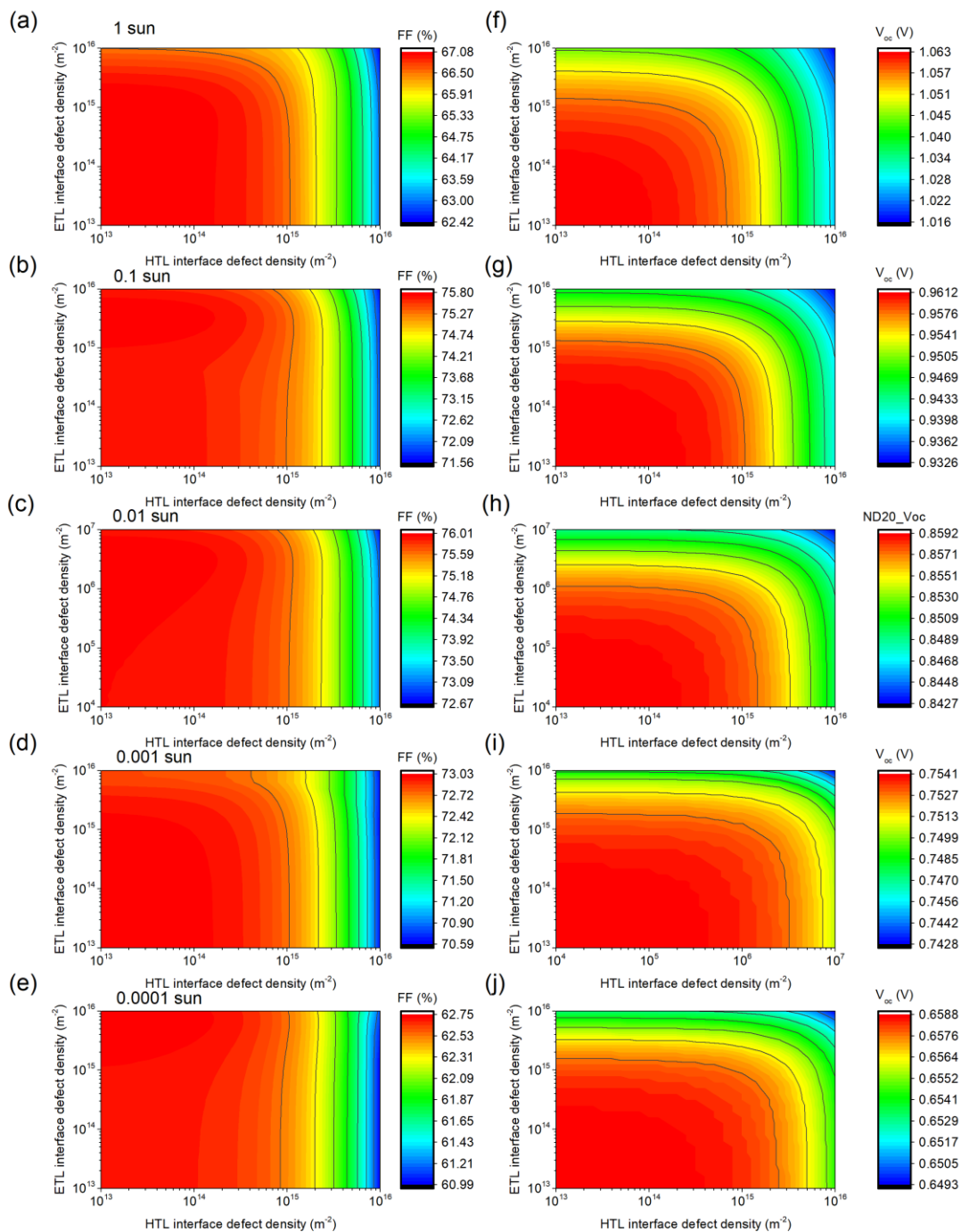


**Figure S5.** 3-D graphs of light intensity-dependent FF and  $V_{oc}$  in the semitransparent PSC with asymmetric interfaces, considering different levels of interface defect densities at HTL and ETL interfaces, for the device with front illumination (through the HTL side).

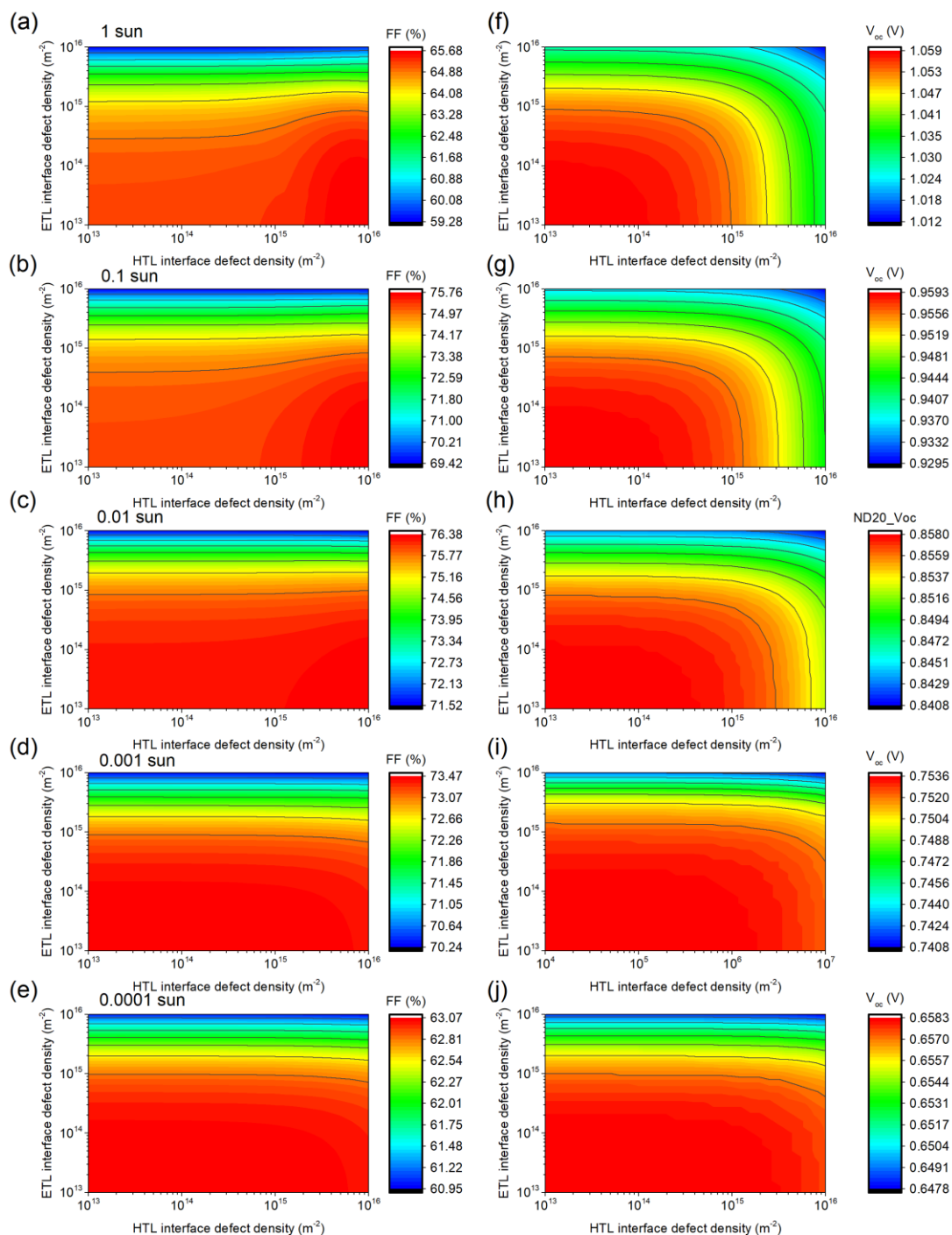


**Figure S6.** 3-D graphs of light intensity-dependent FF and  $V_{oc}$  in the semitransparent PSC with asymmetric interfaces, considering different levels of interface defect densities at HTL and ETL interfaces, for the device with rear illumination (through the ETL side).

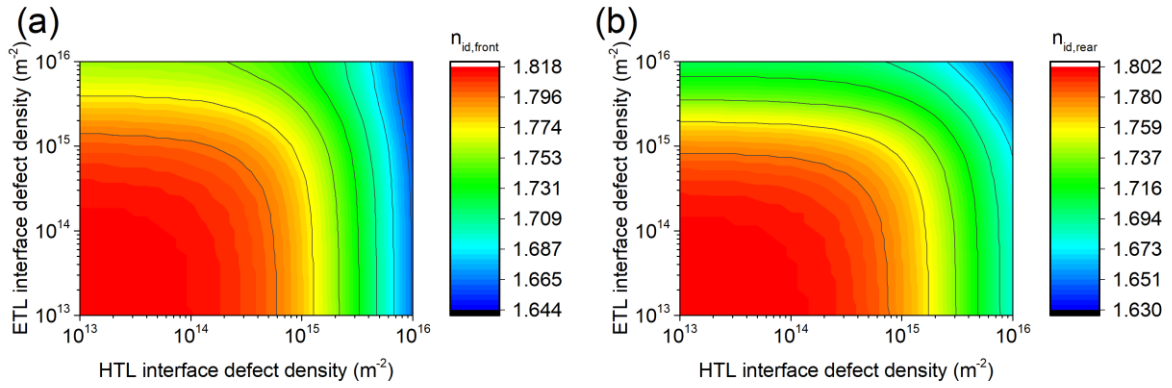


**Figure S7.** 3-D graphs of the ideality factor in semitransparent PSC with asymmetric interfaces, considering different levels of interface defect densities at HTL and ETL interfaces.

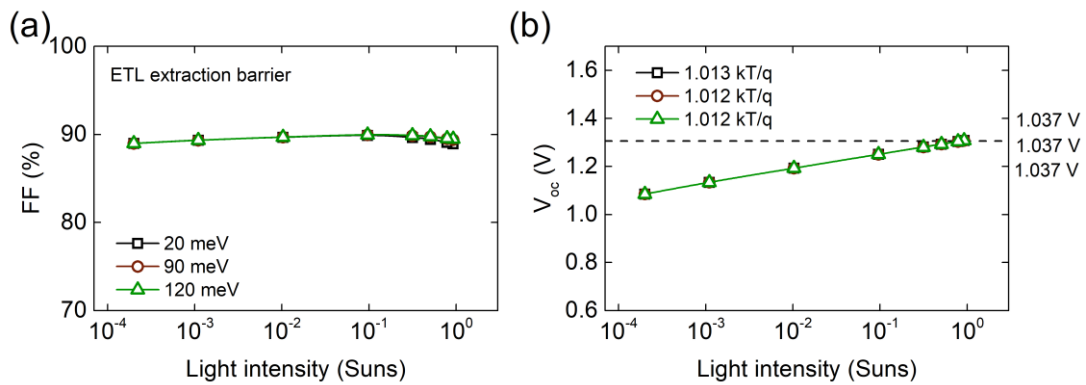


**Figure S8.** Simulated results done without counting done without resistance and recombination losses for (a) FF and (b)  $V_{oc}$  of semitransparent PSCs with front side illumination under different light intensities. The ETL extraction barrier is changed by 20 meV (black square symbol), 90 meV (red circle symbol), and 120 meV (green upper triangle symbol).